Plasmonic antenna array at optical frequency made by nanoapertures

Z. J. Zhang,[1] R. W. Peng,[1,a)] Z. Wang,[1] F. Gao,[1] X. R. Huang,[2] W. H. Sun,[1] Q. J. Wang,[1] and Mu Wang[1]

[1]*National Laboratory of Solid State Microstructures and Department of Physics, Nanjing University, Nanjing 210093, People's Republic of China*

[2]*National Synchrotron Light Source II, Brookhaven National Laboratory, Upton, New York 11973-5000, USA*

(Received 7 July 2008; accepted 10 October 2008; published online 31 October 2008; publisher error corrected 7 November 2008)

We show here that the plasmonic array based on nanoapertures in ultrathin silver film radiates at optical frequency and behaves as an optical antenna array (OAA). The far-field radiation originates from the coherent superposition of plasmonic emissions on each bank of the aperture. The radiation of OAA presents a strong directivity, which depends on the in-plane rotation of aperture array, and on the polarization and incidence angle of the excitation light as well. We suggest that these features have potential applications in photovoltaics, light-emitting devices, and optical sensors. © *2008 American Institute of Physics*. [DOI: 10.1063/1.3010741]

Antennae play an important role as transmitters and receivers of electromagnetic radiation, and are widely applied in the radio frequency and microwave regimes. Recently, the concept of antenna has been extended to the optical frequency. Although there exist two challenges in achieving optical antennae: nanomanufacturing with sufficient precision and identification of specific antenna, designing and fabrication of optical antennae have obtained remarkable achievements very recently. For example, bow-tie antenna,[1] resonant gold dipole antenna,[2] metal nanoparticles, and carbon nanotubes as optical antennae[3] have been experimentally realized. Effective wavelength scaling for optical antennae have also been revealed in theoretical designing.[4] However, most works on optical antenna array (OAA) reported so far focus on electromagnetic radiation of metallic nanorods and nanoparticles, where plasmon resonances[5] are involved.

Since Ebbesen *et al.*[6] reported the extraordinary optical transmission through a two-dimensional array of subwavelength holes perforated on silver film, the investigations on surface plasmons (SPs) have been rekindled in the past decade,[7–10] which offer the potential applications including plasmonic chips, nanolithography, and biophotonics. In this work, we show for the first time that the plasmonic array based on nanoapertures in ultrathin silver film radiates at optical frequency and behaves as an OAA. The far-field emission originates from the coherent superposition of the plasmonic emissions, which relate to the incident light, the localized SPs, and also the propagating SPs.

Experimentally a thin layer of silver 50 nm thick is coated on a piece of optical glass by magnetron sputtering. The array of apertures is milled in the film by focused-ion-beam facility (strata FIB 201, FEI company, 30 keV Ga ions), with a periodicity of the square lattice $a \cong 300$ nm and a diameter of each aperture $d \cong 150$ nm, as shown in Fig. 1(a). The optical transmission spectrum of this structured silver film is measured by a spectrophotometer (PerkinElmer Lambda 900). Figure 1(b) shows the measured optical transmission spectrum of the silver film with aperture array. The main transmission peak appears at $\lambda_0 \cong 615$ nm $\cong 2a$. It is well known that in silver film perforated by the array of subwavelength holes, the periodic array can provide the missing momentum for coupling incoming light to SPs, which leads to the maximum transmission at $\lambda_{max} = (a/(\sqrt{i^2+j^2}))\sqrt{\varepsilon_D \varepsilon_M/(\varepsilon_D+\varepsilon_M)}$. (Here, ε_M and ε_D are the permittivities of the metal and the dielectric, respectively. And i,j are both integers.) In our case, the transmission peak below 500 nm in Fig. 1(b) indeed satisfies the above expression of λ_{max}. However, the main peak at $\lambda_0 \cong 615$ nm in Fig. 1(b) completely deviates from λ_{max}. This feature indicates that the main peak at λ_0 in Fig. 1(b) may not originate from the coupling of the incoming light and SPs; instead, we will show that it comes from the plasmonic emission.

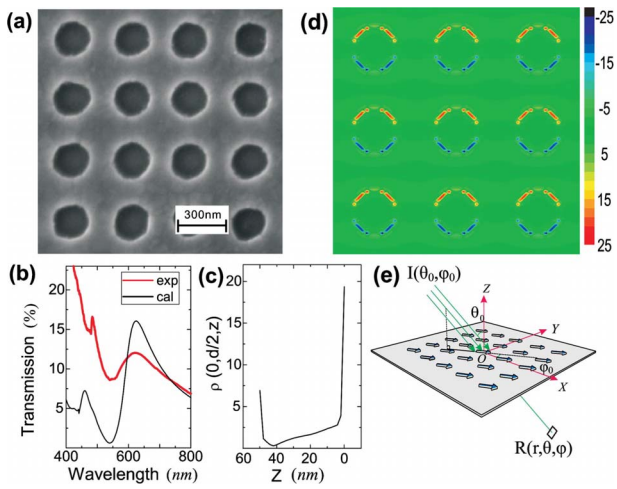

FIG. 1. (Color online) (a) The field-emission scanning electronic microscope image of the array of apertures perforated on 50 nm thick silver film, where the lattice period is about 300 nm and the diameter of the aperture is about 150 nm. (b) The measured and calculated optical transmission spectra of this film in perpendicular incidence. (c) The maxima of calculated charge density at the edge of the aperture. The Z axis is along the growth of silver film and $z=0$ is set at the bottom surface. Here, the wavelength of light ($\lambda_0 \cong 615$ nm) corresponds to the transmission peak. (d) The distribution of charge density at the bottom surface of silver film, which corresponds to the transmission peak at λ_0. (e) A schematic diagram for a planar antenna array of plasmonic dipoles.

a)Author to whom correspondence should be addressed. Electronic mail: rwpeng@nju.edu.cn.

The measured optical transmission spectrum of the silver film with aperture array reasonably agrees with the calculated one [as shown in Fig. 1(b)]. In the calculation, three-dimensional full-vector finite-difference time-domain (FDTD) method is applied.[11] The frequency-dependent permittivity of silver is based on the Lorentz–Drude model.[12] In addition to the optical properties, we have also calculated the charge density distribution[13] in the aperture array at the wavelength λ_0. It is found that the electric charge accumulates at the edge of each aperture on both the top and bottom surfaces of the silver film, and on the bottom surface the charge accumulation is even more evident, as shown in Fig. 1(c). As illustrated in Fig. 1(d), the positive and negative charges accumulate separately on the opposite bank of the aperture [Fig. 1(d)], forming plasmonic dipoles oscillating coherently with the incidence light.

It is interesting to study the optical excitation of the nanohole array. When the incident light illuminates the nanohole array, the localized surface plasmons (LSPs) are excited[14] and serve as electric dipoles. Actually, the dipoles are induced by the local electric field, which includes the following three parts: (i) the incident electric field, (ii) the field created by the other induced dipoles in the array,[15] and (iii) the field contributed by the propagating surface plasmons (PSPs)[7,16] in case that they are excited. Therefore, the electric moment of the nth dipole in the array can be written as

$$\vec{P}_n = \alpha_n \vec{E}_{\parallel}^0 - \alpha_n \sum_{m \neq n} A_{mn} \vec{P}_m + \sum_{m \neq n} c_m \vec{P}_m e^{i\vec{k}_{sp} \cdot \vec{r}_{mn}}. \quad (1)$$

The first term in Eq. (1) is from the in-plane incident field ($\vec{E}_{\parallel}^0$), and the polarizability α_n follows the Clausius–Mossotti relation[17] as $\alpha_n = r^3[1-\varepsilon_M]/[1+2\varepsilon_M]$ for a small spherical vacuum void of radius r in a metal. The second term is from the field created by the other induced dipoles ($A_{mn}\vec{P}_m$, $m \neq n$) in the array, and the electrostatic propagator A_{mn} is equal to $-2/|\vec{r}_{mn}|^3$ for the incident polarization parallel to the line between the dipoles and $1/|\vec{r}_{mn}|^3$ for the perpendicular case. (Here $|\vec{r}_{mn}|$ is the distance between the nth dipole and the mth one.) While the third term is from the PSPs, c_m is the coupling parameter and $\vec{k}_{sp}$ is the wave vector of the PSP. If we only consider the interaction among the nearest dipoles, the electric moment of the nth dipole in a square array can be simplified to $\vec{P}_n \cong \alpha_n \vec{E}_{\parallel}^0/(1-2\alpha_n/a^3 - ce^{ik_{sp}a})$, where a is the lattice period. Hence the local field induces the electric dipole around the nanoaperture, and the dipoles oscillate with the frequency of incidence light. The array of nanoapertures actually performs as a planar antenna array [as shown in Fig. 1(e)]. At some resonant modes, the local field is strong, thus the moments of the dipoles become large enough, and the emission of the dipole array can be received even at the far field.

Based on classical antenna-array theory,[18] we investigate the far-field emission of a rectangle array of $N_x \times N_y$ oscillating dipoles (nanoapertures), which locates at x-y plane and has a spatial periodicity (a_x, a_y). For generality, we let the dipole array being illuminated obliquely with incidence angle θ_0 and in-plane angle ϕ_0 [as shown in Fig. 1(e)]. The far-field receiver locates at $R(r, \theta, \phi)$. (Here $r \gg a_x$ and $r \gg a_y$.) The far-field emission pattern for the planar dipole array has been calculated in both transverse-electric (TE) and transverse-magnetic (TM) incidences, respectively [as shown in Figs. 2(a)–2(c) and Figs. 3(a)–3(c)]. The major features of a planar dipole array can be identified. First, the emission field has a maximum in the case of $\theta = \theta_0$ and $\phi = \phi_0$. Second, the radiation of the dipole array possesses a strong directivity.[18] The directivity is significantly enhanced when the number of dipoles increases in the array. The maximum radiation strength of the planar dipole array exists at the wavelength about the twice of the lattice parameter of the array, i.e., $\lambda_0 \cong 2a_{x(y)}$, in the case of $\theta_0 = 0$ and $\phi_0 = 0$. Obviously, this feature has been demonstrated in our case [as shown in Fig. 1(b)]. Third, the maximum radiation depends

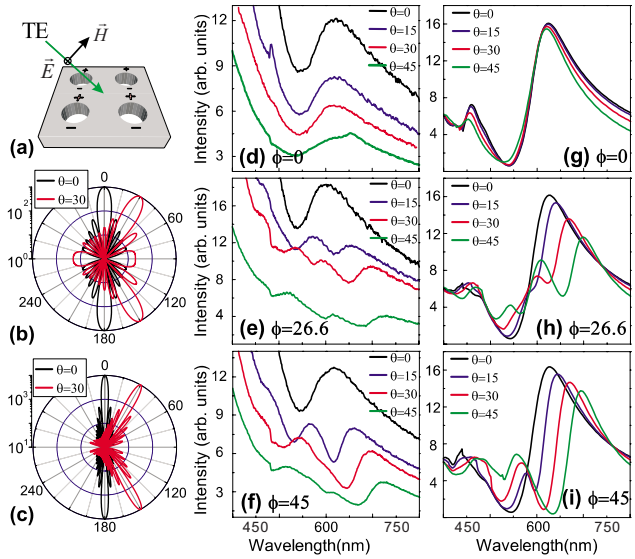

FIG. 2. (Color online) (a) The configuration of TE incidence on the sample described in Fig. 1(a). The calculated far-field E-plane patterns for the arrays of (b) 10×10 dipoles and (c) 20×20 dipoles excited by TE incidence at $\lambda = 600$ nm. The measured [(d)–(f)] and calculated [(g)–(i)] optical spectra detected at the far field $R(r, \theta_0, \phi_0)$, i.e., $\theta = \theta_0$ and $\phi = \phi_0$ [as shown in Fig. 1(e)]. Note that all angles (θ, ϕ) are in degrees.

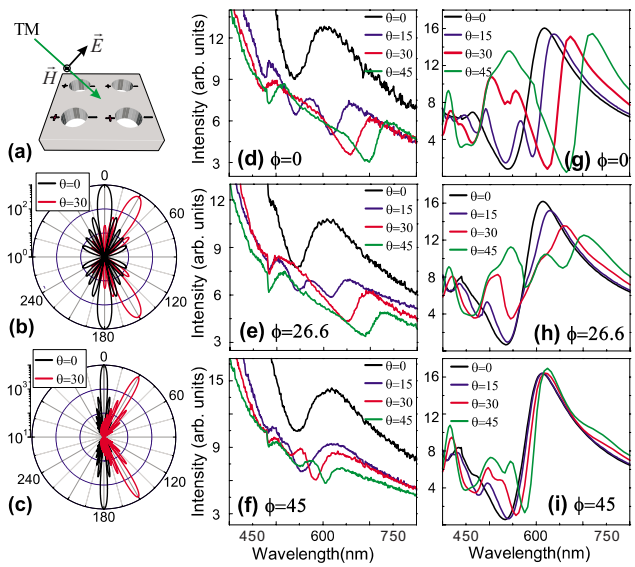

FIG. 3. (Color online) (a) The configuration of TM incidence on the sample described in Fig. 1(a). The calculated far-field E-plane patterns for the arrays of (b) 10×10 dipoles and (c) 20×20 dipoles excited by TM incidence at $\lambda = 600$ nm. The measured [(d)–(f)] and calculated [(g)–(i)] optical spectra detected at the far field $R(r, \theta_0, \phi_0)$, i.e., $\theta = \theta_0$ and $\phi = \phi_0$ [as shown in Fig. 1(e)]. Note that all angles (θ, ϕ) are in degrees.

on the polarization, the angle of incidence light, and also the in-plane rotation of dipole array.

Now we study experimentally the far-field emission of plasmonic array based on the nanoaperture array in the silver film. The square array contains 100×100 holes with period $a\cong300$ nm. The diameter of the hole is $d\cong150$ nm. The light with a TE mode and a TM mode illuminates on the nanoaperture array, respectively. The incidence angle θ_0 varies and the array can be rotated in plane. The optical detector locates at far field $R(r,\theta_0,\phi_0)$, i.e., $\theta=\theta_0$ and $\phi=\phi_0$ [as shown in Fig. 1(e)].

When a TE light illuminates the nanoaperture array on silver film, there is no excitation of PSPs on surface.[7] However, LSPs (Ref. 14) can be excited around each aperture; thereafter, a plasmonic dipole is formed across each nanoaperture. Actually, the dipole is induced by both the incident electric field and the field created by the other induced dipoles in the array. Hence the electric moment of the dipole contains the first two terms in Eq. (1). The far-field emission of the plasmonic array is demonstrated by the measured optical spectra [as shown in Figs. 2(d)–2(f)]. In the case of $\phi_0=0$, the radiation peak appears at $\lambda_0\cong615$ nm$\cong2a$, which remains even if the incidence angle θ_0 is changed [as shown in Fig. 2(d)]. Physically, when TE light obliquely illuminates the nanoaperture array, the incident electric field always lies in plane of the nanoapertures and keeps identically even if the incidence angle varies. As a result, the distribution of plasmonic dipoles in the array remains and the directivity of the radiation is kept at different incidence angles. However, for a nonvanishing ϕ_0, the moment of each plasmonic dipole remains for different incidence angles, yet the array factor[18] varies when the incidence angle is changed. Consequently, the directivity of the dipole antenna array is changed, the maximum radiation shifts to lower frequency, and its intensity decreases as the incidence angle θ_0 is increased, as shown in Figs. 2(e) and 2(f). Numerical calculations based on FDTD method reasonably agree with the measurements [as shown in Figs. 2(g)–2(i)]. The deviation between the experiment and the calculation mainly comes from the fact that the measurements are made at far field; however, the calculations include the near-field contributions in additional to the far-field ones.

Meanwhile, the optical emission of plasmonic array is experimentally observed when the TM mode of electromagnetic wave illuminates the nanoaperture array in the silver film, as shown in Figs. 3(d)–3(f). In this case, the dipole is induced by the incident electric field, the field created by the other induced dipoles in the array, and also the field contributed by the PSPs. The moment of the excited dipole contains all three terms in Eq. (1). Obviously, for $\phi_0=0$, the radiation peak can be found, but maximum radiation redshifts as the incidence angle θ_0 is increased [Fig. 3(d)], which is quite different from that in TE illumination [Fig. 2(d)]. Actually, when the TM light illuminates the aperture array perforated on silver film, both PSPs and LSPs are excited on the surface of silver film. But the in-plane incident field decreases as increasing the incidence angle, which leads to the feature that the moment of each plasmonic dipole is varied for different incidence angles. Hence, the maximum radiation of the plasmonic array redshifts [as shown in Fig. 3(d)]. For a nonvanishing ϕ_0, both the moment of the dipole and the array factor are changed; therefore, the radiation peak also redshifts and the radiation decreases as the incidence angle θ_0 is increased, as shown in Fig. 3(e). A special case occurs at $\phi_0=45°$. As shown in Fig. 3(f), the maximum radiation shifts only slightly when the incidence angle is increased. This phenomenon might come from the fact that PSPs not only change the magnitude of dipoles but also modulate coherent superposition of all dipoles, and then the directivity of the dipole antenna array may not be changed at certain peculiar condition. Numerical calculations of the optical spectra based on FDTD method are shown in Figs. 3(g)–3(i), which are reasonably in agreement with measurements.

In conclusion, we demonstrate in this work a phenomenon that the plasmonic array made by nanoapertures on ultrathin metallic film can radiate as an optical antenna array. Similar radiation behavior of the nanoaperture array can be found at near-infrared regime. These findings provide a new way to construct optical and near-infrared antenna arrays, and may have potential applications in efficiency increase for photovoltaics, light-emitting devices, and optical sensors.

The authors gratefully acknowledge the discussion with Professor Xiang Zhang. This work was supported by grants from the NSFC (Grant Nos. 10625417, 50672035, and 10874068), the MOST of China (Grant Nos. 2004CB619005 and 2006CB921804), and partly by the ME of China and also Jiangsu Province (Grant Nos. NCET-05-0440 and BK2008012).

[1] R. D. Grober, R. J. Schoellkopf, and D. E. Prober, Appl. Phys. Lett. **70**, 1354 (1997); P. J. Schuck, D. P. Fromm, A. Sundaramurthy, G. S. Kino, and W. E. Moemer, Phys. Rev. Lett. **94**, 017402 (2005).
[2] P. Mühlschlegel, H. J. Eisler, O. J. F. Martin, B. Hecht, and D. W. Pohl, Science **308**, 1607 (2005).
[3] J. S. Shumaker-Parry, H. Rochholz, and M. Kreiter, Adv. Mater. (Weinheim, Ger.) **17**, 2131 (2005); K. Kempa, J. Rybczynski, Z. P. Huang, K. Gregorczyk, A. Vidan, B. Kimball, J. Carlson, G. Benham, Y. Wang, A. Herczynski, and Z. F. Ren, *ibid.* **19**, 421 (2007).
[4] L. Novotny, Phys. Rev. Lett. **98**, 266802 (2007).
[5] R. H. Ritchie, Phys. Rev. **106**, 874 (1957); H. S. Zhou, I. Honma, H. Komiyama, and J. W. Haus, Phys. Rev. B **50**, 12052 (1994).
[6] T. W. Ebbesen, H. J. Lezec, H. F. Ghaemi, T. Thio, and P. A. Wolff, Nature (London) **391**, 667 (1998).
[7] W. L. Barnes, A. Dereux, and T. W. Ebbesen, Nature (London) **424**, 824 (2003); C. Genet and T. W. Ebbesen, *ibid.* **445**, 39 (2007).
[8] N. Fang, H. Lee, C. Sun, and X. Zhang, Science **308**, 534 (2005); K. H. Su, Q. H. Wei, and X. Zhang, Appl. Phys. Lett. **88**, 063118 (2006); A. Battula, S. Chen, Y. Lu, R. J. Knize, and K. Reinhardt, Opt. Lett. **32**, 2692 (2007).
[9] Z. H. Tang, R. W. Peng, Z. Wang, X. Wu, Y. J. Bao, Q. J. Wang, Z. J. Zhang, W. H. Sun, and M. Wang, Phys. Rev. B **76**, 195405 (2007).
[10] Y. Alaverdyan, B. Sepúlveda, L. Eurenius, E. Olsson, and M. Käll, Nat. Phys. **3**, 884 (2007).
[11] A. Taflove and S. C. Hagness, *Computational Electrodynamics: The Finite-Difference Time-Domain Method*, 3rd ed. (Artech House, Norwood, 2005).
[12] A. D. Rakic, A. B. Djurisic, J. M. Elazar, and M. L. Majewski, Appl. Opt. **37**, 5271 (1998).
[13] X. R. Huang, R. W. Peng, Z. Wang, F. Gao, and S. S. Jiang, Phys. Rev. A **76**, 035802 (2007).
[14] A. Degiron, H. J. Lezec, N. Yamamoto, and T. W. Ebbesen, Opt. Commun. **239**, 61 (2004).
[15] D. J. Cho, F. Wang, X. Zhang, and Y. Ron Shen, Phys. Rev. B **78**, 121101 (2008).
[16] Y. J. Bao, R. W. Peng, D. J. Shu, M. Wang, X. Li, J. Shao, W. Lu, and N. B. Ming, Phys. Rev. Lett. **101**, 087401 (2008).
[17] B. T. Draine and P. J. Flatau, J. Opt. Soc. Am. A **11**, 1491 (1994).
[18] E. A. Wolff, *Antenna Analysis* (Artech House, Norwood, 1988).